ORIGINAL PAPER

Geostatistical improvements of evapotranspiration spatial information using satellite land surface and weather stations data

Marcelo de Carvalho Alves ·
Luiz Gonsaga de Carvalho · Rubens Leite Vianello ·
Gilberto C. Sediyama · Marcelo Silva de Oliveira ·
Arionaldo de Sá Junior

Abstract The objective of the present study was to use the simple cokriging methodology to characterize the spatial variability of Penman–Monteith reference evapotranspiration and Thornthwaite potential evapotranspiration methods based on Moderate Resolution Imaging Spetroradiometer (MODIS) global evapotranspiration products and high-resolution surfaces of WordClim temperature and precipitation data. The climatic element data referred to 39 National Institute of Meteorology climatic stations located in Minas Gerais state, Brazil and surrounding states. The use of geostatistics and simple cokriging technique enabled the characterization of the spatial variability of the evapotranspiration providing uncertainty information on the spatial prediction pattern. Evapotranspiration and precipitation surfaces were implemented for the climatic classification in Minas Gerais. Multivariate geostatistical determined improvements of evapotranspiration spatial information. The regions in the south of Minas Gerais derived from the moisture index estimated with the MODIS evapotranspiration (2000–2010), presented divergence of humid conditions when compared to the moisture index derived from the simple kriged and cokriged evapotranspiration (1961–1990), indicating climate change in this region. There was stronger pattern of crossed covariance between evapotranspiration and precipitation rather than temperature, indicating that trends in precipitation could be one of the main external drivers of the evapotranspiration in Minas Gerais state, Brazil.

M. de Carvalho Alves (✉)
Soil and Rural Engineering Department,
Federal University of Mato Grosso,
Cuiabá, Brazil
e-mail: marcelocarvalhoalves@gmail.com

M. de Carvalho Alves
e-mail: mdecalves@ufmt.br

L. G. de Carvalho
Engineering Department (DEG),
Federal University of Lavras (UFLA),
Campus, Cx 3037,
CEP 37200-000, Lavras, Minas Gerais, Brazil

L. G. de Carvalho
e-mail: lgonsaga@ufla.br

R. L. Vianello
National Institute of Meteorology,
5o DISME, Avenida do Contorno, n.8159,
Santo Agostinho CEP 30110-051 Minas Gerais, Brazil
e-mail: rubens.vianello@inmet.gov.br

G. C. Sediyama
Agricultural Department, Federal University of Viçosa,
Av P. H. Holfs, Centro,
CEP 36571000, Viçosa, Minas Gerais, Brazil
e-mail: g.sediyama@ufv.br

M. S. de Oliveira
Department of Exact Sciences, UFLA/DEX,
Lavras, Brazil
e-mail: marcelo.oliveira@ufla.br

A. de Sá Junior
Federal Institute of Education,
Science and Technology of the South of Minas Gerais,
Cx 02, km 35, Morro Preto,
CEP 37890-000, Muzambinho, MG, Brazil
e-mail: arionaldojr@hotmail.com

1 Introduction

The evapotranspiration refers to the total loss of water into the atmosphere from the surface of the soil and plants. The simultaneous combination of the soil evaporation and plant transpiration is correspondent to the opposite process of rainfall, also expressed in millimeters (Pereira et al. 1997). The available water for humans and ecosystems in a given region can be approximated by the difference between accumulated precipitation and evapotranspiration (Donohue et al. 2007). The evapotranspiration is a vital component of the water cycle, which includes precipitation, runoff, streamflow, soil water storage, and evapotranspiration (Mu et al. 2009). Land evapotranspiration is a central process in the climate system and a nexus of the water, energy, and carbon cycles, returning about 60 % of annual land precipitation to the atmosphere (Jung et al. 2010).

Evapotranspiration zoning is extremely important for the implantation of infrastructures of water resources, climatic classification, and for the efficiently using of water resources. According to Irmak et al. (2006), accurate and consistent estimates of evapotranspiration in agriculture are also crucial for optimizing crop production at different crop phenological stages, planning for water allocation, scheduling irrigation, evaluating the effects of changing land use on water yields, and assessing the impacts of management practices on environmental quality.

In general, the methodologies most used and recommended to estimate crop water requirements are based on meteorological data (Lemos Filho et al. 2007, 2010). Thus, the evapotranspiration can be estimated by empirical models, semiempirical and physical–mathematical formulation of the evapotranspirative process, using weather variables. The choice of a method depends on the availability of weather data as well as on the accuracy and precision of model estimates for a given region. Therefore, to investigate which method is the best for the characterization of a particular region, it is necessary to make a comparison of different models, observing the quality of the estimates.

The potential evapotranspiration (ETp) can be estimated by Thornthwaite (1948) method in order to represent the water loss process in the soil plant system, using temperature information. Despite the simplicity of this method, it has been demonstrated that temperature is not sufficient as an indication of the energy available for evapotranspiration, considering that, in some regions, the winds, solar radiation, and relative humidity can play an important role in evapotranspiration, but were not considered by this method (Pereira et al. 1997; Allen et al. 1998).

However, in 1990, the methods recommended by Food and Agriculture Organization of the United Nations (FAO) (Doorenbos and Pruitt 1977) concluded that the best evapotranspiration results were obtained by the Penman–Monteith method. It has been subsequently recommended, after some parameterizations, as the standard method to estimate the reference evapotranspiration (Allen et al. 1998; Smith et al. 1990; Smith 1991). In this method, the best evapotranspiration (ETo) estimates were obtained in function of their physic–mathematic formulation of the evapotranspiration process and the greatest number of considered variables, increasing the accuracy of the estimates (Allen et al. 1998). However, the ETo method was restricted due to the requirement of a great number of climatic elements.

Remote sensing can be used to minimize the absence of weather stations in land surface, being recognized as the most feasible means to provide spatially continuous and temporally distributed regional evapotranspiration information on Earth (Mu et al. 2007a,b, 2009, 2011). Remotely sensed data can also be used to monitor surface biophysical variables affecting evapotranspiration, including albedo, biome type, leaf area index, and gross and net vegetation primary production (Mu et al. 2011; Zhao et al. 2005; Zhao and Running 2010).

The radiometric, geometric properties, atmospheric correction, cloud screening, and the high temporal and spatial resolution of the Moderate Resolution Imaging Spetroradiometer (MODIS) products, onboard NASA's Terra and Aqua satellites, provided a significantly improved basis for evapotranspiration monitoring in near real-time and intermediate spatial resolution (Mu et al. 2011). Remotely sensed elevation data obtained from the Shuttle Radar Topography Mission (SRTM) were used to generate high-resolution interpolated climate surfaces of the global land areas using multivariate thin-plate smoothing spline algorithm, enabling to capture environmental variability that can be partly lost at lower resolutions, particularly in mountainous and other areas with steep climate gradients (Hijmans et al. 2005).

When the Earth's surface has distinct spatial properties, the brightness values in imagery constitute a record of the spatial characteristics in the form of texture or pattern. The spatial autocorrelation relationships of a pixel and its neighbors can be used to quantify the spatial pattern in the images using geostatistics (Jensen 2005). Geostatistical interpolation techniques could be used to evaluate the spatial relationships associated with the existing data to create a new, improved systematic grid of values at unsampled locations (Goovaerts 2000). Other applications were related to image classification and the allocation of sampling sites for map accuracy assessment (Atkinson and Curran 1995; Atkinson and Lewis 2000; Curran 1988; Maillard 2003; Woodcock et al. 1988a,b; Chappell 1998).

Global annual evapotranspiration increased from 1982 to 1997, and after that, coincident with the last major El Niño event in 1998, the global evapotranspiration increase seems to have ceased until 2008 (Jung et al. 2010). Large-scale droughts have reduced regional net primary production (NPP), and a drying trend in the Southern Hemisphere has decreased NPP in

that area, counteracting the increased NPP over Northern Hemisphere in the past decade (2000–2009) (Zhao and Running, 2010). The terrestrial gross primary production (GPP) over 40 % of the vegetated land was associated with precipitation, suggesting the existence of missing processes or feedback mechanisms which attenuate the vegetation response to climate (Beer et al. 2010). According to Teuling et al. (2009), in central Europe occurred a strong trend of evapotranspiration correlated with radiation, but in central North America, the correlation was weak.

Spatial correlation among evapotranspiration, precipitation, and temperature in Minas Gerais state is still lacking, and the evidence of evapotranspiration increase in the recent years is a long-standing paradigm in climate research. Considering the existence of a systematic collection of climate elements in macroscale spatial resolution of the National Network of Meteorological Surface Observations (INMET), as well as the existence of remotely sensed meteorology data in high spatial resolution, we aimed to: (1) determine the spatial variability and pattern of the evapotranspiration estimated by FAO Penman–Monteith and Thornthwaite approaches; (2) evaluate the spatial correlation between evapotranspiration, WorldClim precipitation, temperature and MODIS evapotranspiration; and (3) implement evapotranspiration and precipitation surfaces for the climatic classification in Minas Gerais state, Brazil.

2 Methods

2.1 Study area

Minas Gerais presents extensive mountain ranges with different characteristics of moisture (Carvalho et al. 2010) as well as evapotranspiration, solar radiation, relative humidity, and wind speed spatial variability (Lemos Filho et al. 2010). According to the Thornthwaite climatic classification, climatic types ranged from semiarid to superhumid in Minas Gerais (Carvalho et al. 2010). Based on the Köppen climate classification, Minas Gerais was characterized by the major climatic groups A–C, corresponding to tropical rainy, dry, and warm temperate climates. The climate classes were Aw, Am, BSh, Cwa, and Cwb, with Aw, Cwa, and Cwb occupying 99.89 % of the territorial area of the state (Sá Júnior 2011).

2.2 Data description

2.2.1 Satellite land surface data

WorldClim mean air temperature, precipitation, and MODIS evapotranspiration high-resolution land surface data were used to improve the spatial information of the INMET evapotranspiration dataset.

WorldClim dataset Mean air temperature and precipitation land surface data were obtained in Hijmans et al. (2005) and called WorldClim dataset. WorldClim mean air temperature (Temp) (°C) and precipitation (Prec) (mm year^{-1}) high-resolution surfaces were referent to the 1950–2000 period, with 1-km spatial resolution, derived from longitude, latitude, and elevation generated by the SRTM. The thin-plate smoothing spline algorithm implemented in the ANUSPLIN package was used for the multivariate interpolation of the data and presented overall agreement when compared with existing dataset at 10 arc min resolution. When compared to previous global climatologies, the WorldClim dataset presented the advantages of higher spatial resolution, more weather station records, improved elevation data, and more information about the uncertainty of spatial patterns (Hijmans et al. 2005).

MODIS evapotranspiration product The terrestrial evapotranspiration (mm year^{-1}) dataset, from 2000 to 2010 period (1 km spatial resolution), was derived from the Moderate Resolution Imaging Spectroradiometer sensor (ET MODIS), onboard NASA's Terra and Aqua satellites (Mu et al. 2011). The MODIS global evapotranspiration products were the first regular 1-km^2 land surface evapotranspiration dataset for the 109.03 million km^2 global vegetated land areas at an 8-day interval (Mu et al. 2007a,b). The evapotranspiration algorithm was further improved in Mu et al. (2011) by simplifying the calculation of vegetation cover fraction; calculating evapotranspiration as the sum of daytime and nighttime components; adding soil heat flux calculation; improving estimates of stomatal conductance, aerodynamic resistance, and boundary layer resistance; separating dry canopy surface from the wet; and dividing soil surface into saturated wet surface and moist surface. The improved evapotranspiration algorithm had satisfactory performance in generating global evapotranspiration data products, providing critical information on global terrestrial water and energy cycles and environmental changes (Mu et al. 2011).

2.2.2 Weather stations

The annual evapotranspiration estimates were obtained from primary data collected by the national network of surface meteorological observations of the National Institute of Meteorology (INMET), represented by 39 weather stations located in Minas Gerais and and surrounding states of Distrito Federal (DF), Goiás (GO), Bahia (BA), Espírito Santo (ES), Rio de Janeiro (RJ), São Paulo (SP), and Mato Grosso do Sul (MS), presented in the Climatological Normals, from 1961 to 1990 period (Brasil 1992) (Fig. 1).
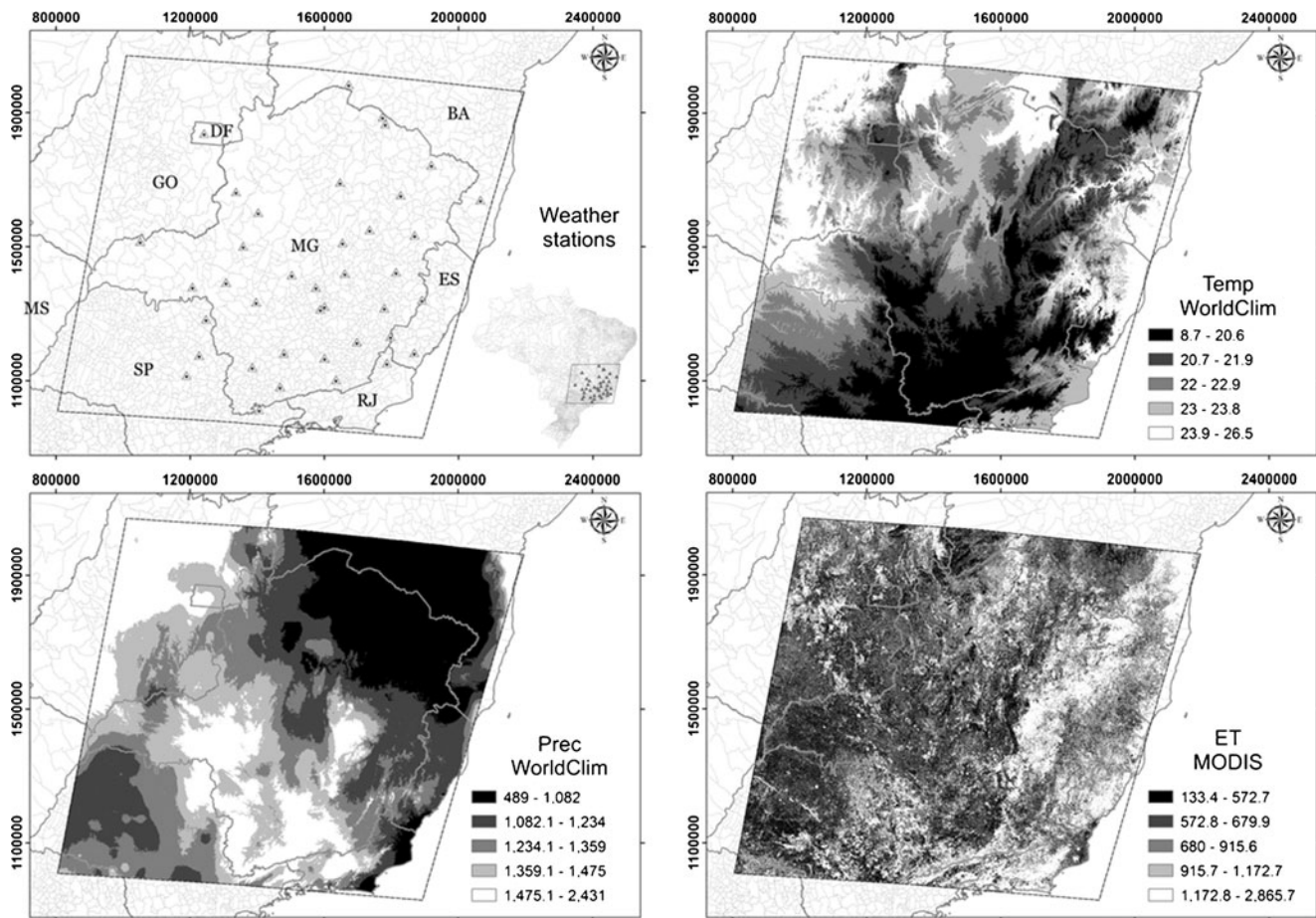
Fig. 1 Input INMET dataset used to perform simple cokriging for evapotranspiration spatial characterization in Minas Gerais and surrounding states (1961–1990) (*top-left panel*), WorldClim mean air temperature (*Temp*) (°C) and precipitation (*Prec*) (mmyear^{-1}) high- resolution surfaces (1950–2000) (*top-right and bottom-left panels*), and the MODIS terrestrial evapotranspiration (mmyear^{-1}) (2000– 2010) (*bottom-right panel*)

Evapotranspiration calculation Despite the FAO Penman– Monteith method is adopted, in conceptual terms, as an evapo- transpiration estimator, commonly applied in irrigation man- agement, in the context of the present study, this method was considered an estimator of the potential evapotranspiration.

The reference evapotranspiration was estimated by the FAO Penman–Monteith method from monthly data of mean, maximum and minimum air temperature, atmospheric pressure, sunlight, relative humidity and wind. The model adopted for the estimation of evapotranspiration was defined by (Allen et al. 1998):

$$ETo = \sum_{i=1}^{12} \left[\frac{s}{s+\gamma^*} (Rn - G) \frac{1}{\lambda} + \frac{\gamma 900}{(s+\gamma*)(T+273)} U_2(es - ea) \right] NDM \tag{1}$$

where,

ETo is the reference evapotranspiration (mmmonth^{-1}), i refers to number of the month in the year, γ is the psico- metric coefficient (kPa°C^{-1}), s is the slope vapor pressure curve saturation (kPa°C^{-1}), γ^* is the modified psicometric coefficient (kPa°C^{-1}), Rn is the balance radiation on the crop surface (MJm^{-2}day^{-1}), G is the flow of heat in the soil (MJ m^{-2}day^{-1}), λ is the latent heat of evaporation (MJkg^{-1}), T is the mean temperature of the air (°C), U_2 is the wind speed in the height of 2 m (ms^{-1}), es is the pressure of saturation of water vapor (kPa), and ea is the actual vapor pressure of water (kPa). The equations used to estimate the parameters of FAO Penman–Monteith equation were presented by Allen et al. (1998) and Pereira et al. (1997). After estimating the ETo for each month, it was proceeded the sum of all months to generate a value of annual evapotranspiration (mmyear^{-1}).

The potential evapotranspiration estimated based on Thornthwaite (1948) and Thornthwaite and Mather (1955), was obtained by:

$$ETp = \sum_{i=1}^{12} \left[16 \left(\frac{10T}{I} \right)^a \right] FC \tag{2}$$

where ETp is the potential evapotranspiration (mm month^{-1}), n refers to number of the month in the year, T is the mean temperature of the air (°C), I is the annual calorific index, a is the index obtained as a cubic function of I, FC is the factor of correction regarding the month and maximum insolation (N). The equations used to estimate the parameters of the equation of Thornthwaite were derived from Thornthwaite (1948). After estimating the ETp for each month, it was proceeded the sum of all months to generate a value of annual potential evapotranspiration (mmyear^{-1}).

After obtaining the evapotranspiration values for each location, nonspatial exploratory analysis of minimum, mean, maximum values, standard deviation, and kurtosis were used to characterize the climate of Minas Gerais and surrounded states based on the evapotranspiration estimated by the Penman–Monteith and Thornthwaite methods (mmyear^{-1}). The same analysis was also applied to other explanatory variables mean air temperature (°C), precipitation (mmyear^{-1}), Thornthwaite humidity index (Carvalho et al. 2010), and elevation derived from the same INMET climatological stations, 1961–1990 period.

Quintile spatial exploratory analysis were used to characterize the climate of Minas Gerais and surrounded states by circle plots of the evapotranspiration estimated by the Penman–Monteith and Thornthwaite methods (mmyear^{-1}), and the explanatory variables mean air temperature (°C), precipitation (mmyear^{-1}), Thornthwaite humidity index (Carvalho et al. 2010), and elevation, derived from INMET climatological stations, 1961–1990 period.

After exploratory data analysis, it was proceeded the simple cokriging geostatistical analysis (Isaaks and Srivastava 1989; Chilès and Delfiner 2008; Wackernagel 2003), in order to characterize the spatial dependency magnitude and structure of the data and to make spatial prediction at unsampled locations, based in the measurement of the data spatial continuity and variability.

2.3 Geostatistical modeling

2.3.1 Measures of spatial continuity and variability

Covariance function Covariance could be used to characterize the structure and magnitude of spatial dependence of the evapotranspiration (Goovaerts 1997).

The covariance between data values separated by a vector h was computed as:

$$C(h) = \frac{1}{N(h)} \sum_{i=1}^{N(h)} z(x_i)z(x_i + h) - m(h)m(x_i + h) \quad (3)$$

where,

$$m(h) = \frac{1}{N(h)} \sum_{i=1}^{N(h)} z(x_i) \quad (4)$$

$$m(x_i + h) = \frac{1}{N(h)} \sum_{i=1}^{N(h)} z(x_i + h) \quad (5)$$

$N(h)$ is the number of data pairs within the class of distance and direction, and $m(h)$ and $m(x_i+h)$ are the means of the corresponding tail and head values (lag means). The covariance was computed for different lags, h_1, h_2, …h_n, and the ordered set of covariances $C(h_1),C(h_2),…C(h_n)$, generated the experimental autocovariance function or the experimental covariance function.

Variogram Unlike the covariance and correlation functions, which are measures of similarity, the experimental variogram $\gamma(h)$ measured the average dissimilarity between evapotranspiration data separated by a vector h. The variogram was computed as half the average squared difference between the components of every data pair (Goovaerts 1997):

$$\gamma(h) = \frac{1}{2N(h)} \sum_{i=1}^{N(h)} \left[z(x_i) - z(x_i + h)\right]^2 \quad (6)$$

where, $z(x_i) - z(x_i + h)$ is an h increment of attribute z.

The variogram was applied to the evapotranspiration data estimated by Penman–Monteith and Thornthwaite methods, to study the structure, magnitude, and spatial variability of the evapotranspiration estimated by FAO Penman–Monteith and Thornthwaite approaches, for the 1961–1990 period.

Crossed covariance function Crossed covariance functions were used to characterize the structure and magnitude of spatial dependence of the evapotranspiration estimated by FAO Penman–Monteith or Thornthwaite approaches, for the 1961–1990 period, with the WorldClim mean air temperature and precipitation high-resolution surfaces from 1950 to 2000, as well as the MODIS evapotranspiration product from 2000 to 2010 period. The crossed covariance functions between the variables and co-variables were performed as (Goovaerts 1997):

$$C(h) = \frac{1}{N(h)} \sum_{i=1}^{N(h)} z_i(x_i)z_j(x_i + h) - m_i(h)m_j(h) \quad (7)$$

where

$$m_i(h) = \frac{1}{N(h)} \sum_{i=1}^{N(h)} z_i(x_i) \tag{8}$$

$$m_j(h) = \frac{1}{N(h)} \sum_{i=1}^{N(h)} z_j(x_i + h) \tag{9}$$

$N(h)$ is the number of data pairs within the class of distance and direction, and $m_i(h)$ and $m_j(h)$ are the means of tail z_i values and head z_j values related to two different attributes, z_i and z_j, respectively. The covariance can be computed for different lags, $h_1, h_2, \ldots h_n$, and the ordered set of crossed covariances $C_{ij}(h_1), C_{ij}(h_2), \ldots C_{ij}(h_n)$, is the experimental crossed covariance function.

Crossed variogram The crossed variogram, when necessary, was computed as (Goovaerts 1997):

$$\gamma_{ij}(h) = \frac{1}{2N(h)} \sum_{i=1}^{N(h)} \left[z_i(x_i) - z_i(x_i + h)\right] \left[z_j(x_i) - z_j(x_i + h)\right] \tag{10}$$

Unlike the cross covariance or cross correlogram, the cross semivariogram is symmetric in i, j and $(h, -h)$; interchanging i and j or substituting $-h$ for h makes no difference in the expression 10.

2.3.2 Parameter estimation

Theoretical covariogram models were estimated by the weighted least squares method (Cressie 1985), with spherical model parameters (Chilès and Delfiner 2008):

$$Spherical\ model: C(h) = C_0 + C \begin{cases} 1 - \frac{3h}{a} + \frac{1}{2}\frac{h^3}{a^3} & if \quad h \leq a \\ 0 & if \quad h \geq a \end{cases} \tag{11}$$

where C_0 is the nugget variance, C is the partial sill, $C_0 + C$ equals the sill, a is the range, and h is the lag distance.

2.3.3 Spatial prediction

Simple kriging: accounting for a single attribute estimation After the experimental variogram determination and parameter estimation, the simple kriging method interpolation was used to estimate the evapotranspiration estimated by FAO Penman–Monteith or Thornthwaite approaches, for the 1961–1990 period, at 1,000-m spatial resolution in Minas Gerais state and boundary regions.

The modeling of the trend component $m(x)$ as a known stationary mean m allows to write the linear estimator as a linear combination of the $n(x)$ random variables $Z(x_i)$ and the mean value m (Goovaerts 1997):

$$\begin{aligned} Z_{sk}^*(x) &= \sum_{i=1}^{n(x)} \lambda_i^{sk}(x)[Z(x_i) - m] + m \\ &= \sum_{i=1}^{n(x)} \lambda_i^{sk}(x)Z(x_i) + \left[1 - \sum_{i=1}^{n(h)} \lambda_i^{sk}(x)\right]m \end{aligned} \tag{12}$$

where $n(x)$ weights $\lambda_i^{sk}(x)$ are then determined such as to minimize the error variance $\sigma_E^2(x) = Var[Z_{sk}^*(x) - Z(x)]$ under the unbiasedness constraint that $E[Z^*(x) - Z(x)] = 0$.

The simple kriging estimator is already unbiased since the error mean is equal to zero:

$$E[Z_{sk}^*(x) - Z(x)] = m - m = 0 \tag{13}$$

Using matrix notation, the simple kriging system can be written as (Goovaerts 1997):

$$K_{sk}\lambda_{sk}(x) = k_{sk} \tag{14}$$

where K_{sk} is the $n(x) \times n(x)$ matrix of data covariances:

$$K_{sk} = \begin{bmatrix} C(x_1 - x_1) & \ldots & C(x_1 - x_{n(x)}) \\ \vdots & \vdots & \vdots \\ C(x_{n(x)} - x_1) & \ldots & C(x_{n(x)} - x_{n(x)}) \end{bmatrix} \tag{15}$$

$\lambda_{sk}(x)$ is the vector of simple kriging weights, and k_{sk} is the vector of data-to-unknown covariances:

$$\lambda_{sk} = \begin{bmatrix} \lambda_1^{sk}(x) \\ \vdots \\ \lambda_{n(x)}^{sk}(x) \end{bmatrix} \qquad k_{sk} = \begin{bmatrix} C(x_1 - x) \\ \vdots \\ C(x_{n(x)} - x) \end{bmatrix} \tag{16}$$

The kriging weights required by the simple kriging estimator are obtained by multiplying the inverse of the data covariance matrix by the vector of data-to-unknown covariances:

$$\lambda_{sk}(x) = K_{sk}^{-1}k_{sk} \tag{17}$$

The matrix formulation of the simple kriging variance is correspondingly

$$\sigma_{sk}^2(x) = C(0) - \lambda_{sk}^T(x)k_{sk} = C(0) - k_{sk}^T K_{sk}^{-1}k_{sk} \tag{18}$$

The covariance function matrix and variogram matrix are related by:

$$\begin{aligned} \Gamma(h) &= C(0) - \frac{1}{2}[C(h) + C(-h)] \\ &= C(0) - C(h),\ if\ lag\ effect\ is\ ignored. \end{aligned} \tag{19}$$

where the matrix $C(0)$ is the traditional variance-covariance matrix.

Log transformation and first trend was applied to the evapotranspiration estimated by FAO Penman–Monteith and Thornthwaite approaches. The trend order was defined

according to the minor kriging standard error. Polynomials were used to model the trend.

The first order trend in R^2 was:

$$m(x) = m(x,y) = a_o + a_1 x + a_2 y + a_3 xy \tag{20}$$

where (x, y) are the coordinates of the location x and a_o, a_1, …, a_n are the parameters.

The transformed evapotranspiration were back-transformed to the original scale to generate the spatial variability maps.

Simple cokriging: accounting for a secondary information The simple cokriging was used to characterize the dependency of spatial magnitude and structure of the evapotranspiration influenced by the WorldClim temperature, precipitation and MODIS evapotranspiration.

After fitting the crossed covariance functions, the simple cokriging method was used to interpolate the data. The simple cokriging estimator was presented here considering a single secondary attribute z_2. Modeling the primary and secondary trend components $m_1(x)$ and $m_2(x)$ as stationary means m_1 and m_2, the linear estimator was (Goovaerts 1997):

$$Z^{(1)*}_{sck}(x) - m_1 = \sum_{i1=1}^{n_1(x)} \lambda^{sck}_{i1}(x)[Z_1(x_{i1}) - m_1]$$

$$+ \sum_{i2=1}^{n_2(x)} \lambda^{sck}_{i2}(x)[Z_2(x_{i2}) - m_2] \tag{21}$$

where the $Z^{(1)*}_{sck}(x)$ is the simple cokriging estimator of the primary attribute z_1 at the location x. The superscripted (1) imply that data locations were not the same from one variable to another. The $[n_1(x)+n_2(x)]$ cokriging weights are determined such as to ensure unbiasedness and minimum error variance. Unbiasedness is guaranteed by:

$$E\left\{Z^{(1)*}_{sck}(x) - Z_1(x)\right\} = \sum_{i1=1}^{n_1(x)} \lambda^{sck}_{i1}(x)[E\{Z_1(x_{i1}) - m_1\}]$$

$$+ \sum_{i2=1}^{n_2(x)} \lambda^{sck}_{i2}(x)[E\{Z_2(x_{i2}) - m_2\}]$$

$$+ [m_1 - E\{Z_1(x)\}] = 0 \tag{22}$$

Considering a single secondary attribute, the matrix notation of the simple cokriging system is written (Goovaerts 1997):

$$K_{sck}\lambda_{sck}(x) = k_{sck} \tag{23}$$

with

$$K_{sck} = \left\{ \begin{bmatrix} C_{11}(x_{\alpha 1} - x_{\beta 1}) \end{bmatrix} \begin{bmatrix} C_{12}(x_{\alpha 1} - x_{\beta 2}) \end{bmatrix} \\ \begin{bmatrix} C_{21}(x_{\alpha 2} - x_{\beta 1}) \end{bmatrix} \begin{bmatrix} C_{22}(x_{\alpha 2} - x_{\beta 2}) \end{bmatrix} \right\} \tag{24}$$

$$\lambda_{sck}(x) = \left\{ \begin{bmatrix} \lambda^{sck}_{\beta 1}(x) \end{bmatrix}^T \\ \begin{bmatrix} \lambda^{sck}_{\beta 2}(x) \end{bmatrix}^T \right\}$$

$$, k_{sck} = \left\{ \begin{bmatrix} C_{11}(x_{\alpha 1} - x) \end{bmatrix}^T \\ \begin{bmatrix} C_{21}(x_{\alpha 2} - x) \end{bmatrix}^T \right\} \tag{25}$$

where $\left[C_{ij}(x_{\alpha i} - x_{\beta j})\right]^T$ is the $n_i(x) \times n_j(x)$ matrix of data auto and crossed covariances, $\left[\lambda^{sck}_{\beta 1}(x)\right]^T$ is an $n_i(x) \times 1$ vector of cokriging weights, and $\left[C_{i1}(x_{\alpha i} - x)\right]^T$ is an $n_i(x) \times 1$ vector of data-to-unknown auto and crossed covariances. The cokriging weights are obtained by multiplying the inverse of matrix K_{sck} by the vector K_{sck}:

$$\lambda_{sck}(x) = K^{-1}_{sck} k_{sck} \tag{26}$$

The simple cokriging variance is then computed as:

$$\sigma^2_{sck}(x) = C_{11}(0) - \lambda^T_{sck}(x) k_{sck}$$

$$= C_{11}(0) - k^T_{sck} K^{-1}_{sck} k_{sck} \tag{27}$$

If primary and secondary variables are uncorrelated, the simple cokriging estimator reverts to the simple kriging estimator. Both simple kriging and simple cokriging estimator are exact interpolators, honoring the primary data at their locations.

Log transformation and third trend was applied to the evapotranspiration estimated by FAO Penman–Monteith and Thornthwaite approaches. The trend order was defined according to the minor kriging standard error. Polynomials were used to model the trend.

The third order trend in R^2 was:

$$m(x) = a_o + a_1 x + a_2 y + a_3 x^2 + a_4 y^2 + a_5 xy$$

$$+ a_6 x^3 + a_7 y^3 + a_8 x^2 y + a_9 xy^2 \tag{28}$$

where (x, y) are the coordinates of the location x and a_o, a_1, …, a_n are the parameters.

Similarly to the simple kriging, the transformed data were back-transformed to the original scale to generate the cokriging spatial variability maps.

2.3.4 Assessment of spatial uncertainty

Simple kriging and cokriging predictions were evaluated using cross-validation analyses. Cross-validation is a powerful validation technique used to check the performance of the models. It consists of removing data, on at a time, and then trying to predict it. The predicted values can be compared to the observed values in order to assess how well the prediction is working, based on self-consistency and lack of bias (Isaaks and Srivastava 1989; Cressie 1993; Goovaerts 1997; Chilès and Delfiner 2008; Burrough and McDonnell 1998).

The simple kriging and cokriging standard deviation is the square root of the kriging and cokriging variance, respectively, providing the error associated with the estimator (Diggle and Ribeiro 2007):

$$SE(x) = \sqrt{Var[Z^*(x)|Z(x)]} \qquad (29)$$

If the nugget is 0, the prediction standard error would have been exactly zero at each sampling locations and the predicted surface $Z^*(x)$ would have interpolated the observed responses $Z(x)$.

Notice that the standard error does not depend on the values of the data but only on their locations (Chilès and Delfiner 2008).

The root mean square prediction error indicated how closely the model predicted the measured values:

$$\sqrt{\frac{\sum\limits_{i=1}^{n} [Z^*(x) - Z_i(x)]^2}{n}} \qquad (30)$$

The average standard errors, representing the average of the prediction standard errors, were defined by:

$$\sqrt{\frac{\sum\limits_{i=1}^{n} \hat{\sigma}^2(x_i)}{n}} \qquad (31)$$

The mean standardized prediction errors were defined by:

$$\frac{\sum\limits_{i=1}^{n} \left[Z^*(x) - Z_i(x)\right]/\hat{\sigma}(x_i)}{n} \qquad (32)$$

The root mean square standardized prediction errors were defined by:

$$\sqrt{\frac{\sum\limits_{i=1}^{n} \{[Z^*(x) - Z_i(x)]/\hat{\sigma}(x_i)\}^2}{n}} \qquad (33)$$

where $Z^*(x)$ was the simple kriging or cokriging estimation, $Z_i(x)$, the observed value, $\hat{\sigma}(x_i)$, the prediction standard error for x_i location. Considering an ideal cokriging performance, mean standardized prediction errors should be 0 and root-mean square standardized prediction errors should be 1 (Cressie 1993). If the root mean squared standardized error is greater than one, the variability in the predictions is been underestimated. If the root mean square standardized error is less than one, the variability in the predictions is been overestimated

After interpolate the values of ETo and ETp, prediction maps in raster format were generated in spatial resolution of 1 km², making possible the assessment of evapotranspiration variability in mesoclimatic scale. Prediction standard error maps were also generated, in order to evaluate the error magnitude across the studied area caused by the interpolation technique.

2.4 Evapotranspiration implementation for the moisture index calculation

Thornthwaite annual moisture index was commonly used to characterize climates (Thornthwaite and Mather 1955; Willmott and Feddema 1992) and other aspects of the environment such as vegetation (Mather and Yoshioka 1968). When Thornthwaite and Mather's (1955) expression is integrated over the average year, $S \rightarrow \max[(P - E), 0]$, and the moisture index (I_m) becomes (Willmott and Feddema 1992):

$$I_m = 100\left(\frac{P}{E^o} - 1\right) \qquad (30)$$

where S is the moisture surplus, P is the precipitation, E is the actual evapotranspiration, and E^o is the potential evapotranspiration.

Different moisture index products were generated based on map algebra calculation in GIS, using WorldClim precipitation (Prec WorldClim) and the different evapotranspiration surfaces: simple kriging Penman–Monteith evapotranspiration (ETo sk), simple kriging Thornthwaite evapotranspiration (ETp sk), simple cokriging Penman–Monteith evapotranspiration (ETo sck), simple cokriging Thornthwaite evapotranspiration (ETp sck), and MODIS evapotranspiration (ET MODIS).

The algebra calculations were performed as:

$$I_m\,ETo_{sk} = 100\left(\frac{Prec\,WorldClim}{ETo\,sk} - 1\right) \qquad (31)$$

$$I_m ETp_{sk} = 100\left(\frac{Prec\,WorldClim}{ETp\,sk} - 1\right) \qquad (32)$$

$$I_m ETo_{sck} = 100\left(\frac{Prec\,WorldClim}{ETo\,sck} - 1\right) \qquad (33)$$

$$I_m ETp_{sck} = 100\left(\frac{Prec\,WorldClim}{ETp\,sck} - 1\right) \qquad (34)$$

$$I_m ET\,MODIS = 100\left(\frac{Prec\,WorldClim}{ET\,MODIS} - 1\right) \qquad (35)$$

3 Results

3.1 Exploratory data analysis

Using the primary data collected by the national network of surface meteorological observations of the National Institute of Meteorology (INMET), represented by 39 weather stations located in Minas Gerais and surrounding states, presented in the Climatological Normals, from 1961 to 1990 period, it was possible to determine the evapotranspiration values using FAO Penman–Monteith and Thornthwaite methods. Examining the preliminary investigation of nonspatial aspects of the analyzed variables, it was observed that ETo and ETp presented similar statistical values, but ETo presented higher kurtosis, minimum, mean, and maximum values (Table 1).

The humidity index ranges indicated the occurrence of different climate types in the evaluated weather stations. Mean air temperature, precipitation, and altitude also presented different magnitude values, indicating spatial variation between the studied stations. The dataset derived from high spatial resolution data, presented low kurtosis values and the ranges were, in general, within acceptable range values, considering that the information collected by the sensor covered a much wider range than that collected by the weather stations. The values of kurtosis below 1 indicates symmetry and does not suggest any obvious outliers, but data transformation could add some support to the use of a Gaussian model as an approximation for these data (Table 1).

The first stage in spatial exploratory data analysis is simply to plot the response data in relation to their locations, for example, using a circle plot. Quintile spatial exploratory plots of the ETo, ETp, and the explanatory variables mean air temperature, precipitation, Thornthwaite humidity index, and elevation, derived from INMET climatological stations,

1961–1990 period, enabled to observe spatial correlation between the studied variables. Observing the north–south direction, it was possible to verify positive spatial correlation between evapotranspiration and temperature, as well as negative spatial correlation between evapotranspiration and precipitation, humidity index, and elevation (Fig. 2). Careful inspection of this plot revealed spatial trends, suggesting the need to include a trend surface model for a spatially varying mean, considering that was something special about the north–south direction, related to the physical environment dependence on longitude, latitude, and altitude.

3.2 Measures of spatial continuity, variability, and parameter estimation

Circle plots can be difficult, especially when analyzing small dataset, to distinguish between a spatially varying mean response and correlated spatial variation about a constant mean. Visual assessment of spatial correlation from a circle plot was also difficult. For a sharper assessment, a useful exploratory tool was the empirical variogram (Diggle and Ribeiro 2007).

Variograms, covariance functions, and crossed covariance functions enabled to characterize the spatial variability of ETo and ETp, as well as the spatial correlation of these variables with high-resolution surfaces of temperature, precipitation, and MODIS ET. The choice on the transformation type and order of trend removal was chosen observing the cross validation results. The log transformation was chosen for all the evaluated variables. The third order of trend removal was adopted for the variables submitted to the simple cokriging analysis and, the first order, to the simple kriging analysis. The spherical model, with weighted least square fit, was useful to define parameters for the spatial prediction. The range values were 185,418.1 m, except for the ETo submitted to the simple kriging, with the range of

Table 1 Nonspatial exploratory analysis used to characterize the climate of Minas Gerais and surrounded states based on the Penman–Monteith (ETo) and Thornthwaite methods (ETp) (mmyear^{-1}) evapotranspiration, and the explanatory variables mean air temperature (Temp) (°C), precipitation (Prec) (mmyear^{-1}), Thornthwaite humidity index, and elevation (m), derived from the INMET climatological stations (1961–1990), as well as the high spatial resolution variables derived from the Worldclim data set of temperature (WorldClim Temp), precipitation (WorldClim Prec) (1950–2000) and the MODIS evapotranspiration product (ET MODIS) (2000–2010)

Statistics	Variables								
	ETo	Etp	Temp	Prec	Humidity Index	Elevation	WorldClim Temp	WorldClim Prec	ET MODIS
Number of data	39.0	39.0	39.0	39.0	39.0	39.0	1,465,867.0	1,173,640.0	1,173,640.0
Minimum	795.9	677.2	13.4	749.8	−52.3	77.5	8.7	489.0	133.4
Maximum	1,574.4	1,385.6	25.0	1,783.1	124.3	1578.8	26.5	2,431.0	2,865.6
Mean	1,129.5	1,036.2	21.2	1319.9	20.8	721.7	22.1	1,272.8	855.4
Standard Deviation	160.6	171.0	2.4	265.8	35.1	325.1	1.8	248.1	309.3
Kurtosis	1.7	−0.6	1.8	−0.6	1.2	0.5	0.0	0.0	-0.3
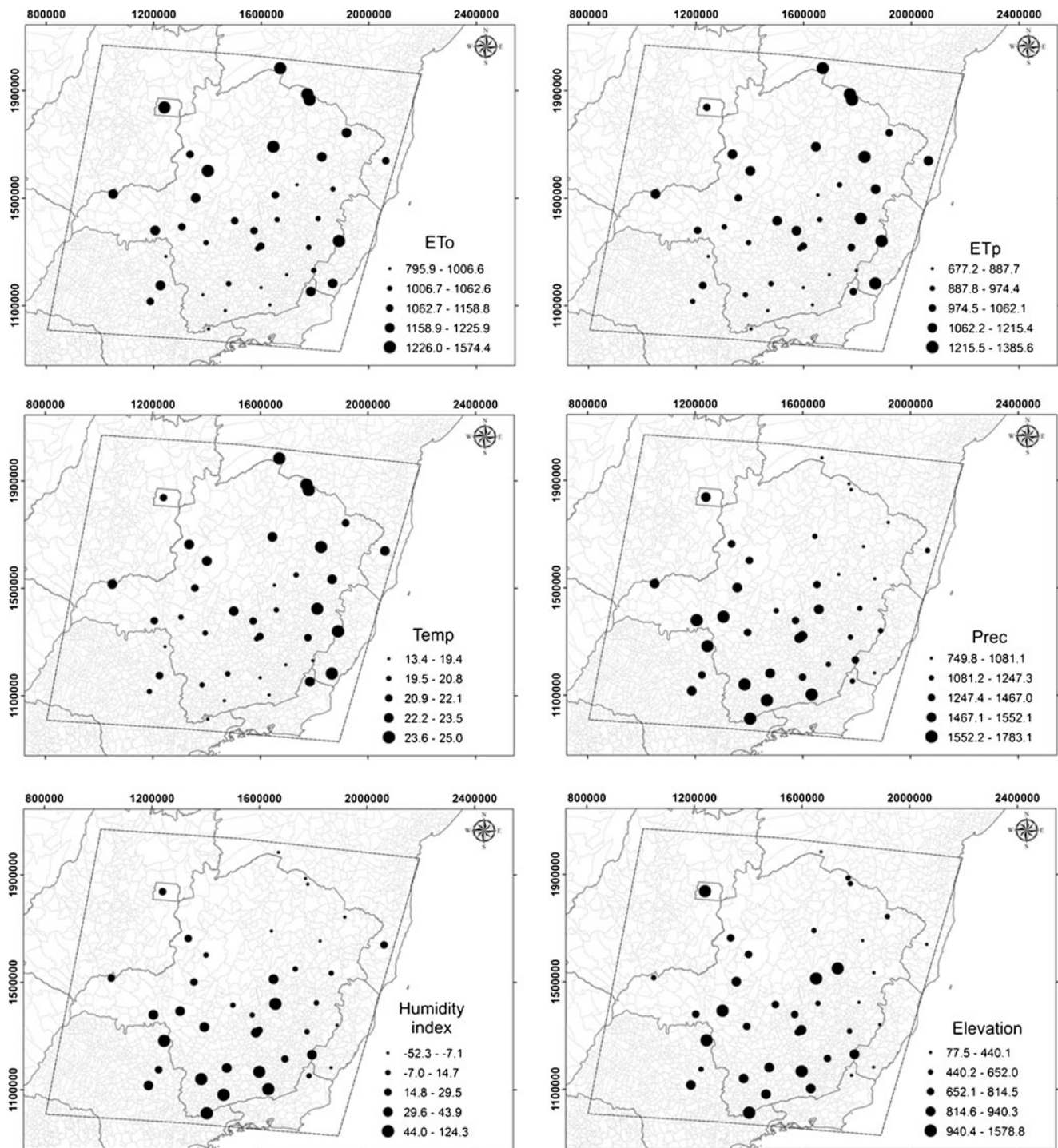
Fig. 2 Quintile spatial exploratory analysis used to characterize the climate of Minas Gerais and surrounded states by circle plots of the evapotranspiration estimated by the Penman–Monteith (*ETo*) and Thornthwaite methods (*ETp*) (mm year^{-1}), and the explanatory variables mean air temperature (*Temp*) (°C), precipitation (*Prec*) (mm year^{-1}), Thornthwaite humidity index, and elevation (m), derived from INMET climatological stations (1961–1990)

253,003.5 m (Table 2). The solid line of the models followed the binned and averaged values of the variograms, covariance, crossed covariance in the simple kriging (Fig. 3), and simple cokriging models (Figs. 4 and 5), with typical behavior of stationary spatially correlated process. ETp and WorldClim temperature presented stronger pattern of spatial crossed covariance than ETo. ETo and MODIS evapotranspiration presented stronger pattern of spatial

Table 2 Theoretical variograms, covariance, crossed covariance parameters used to characterize the structure and magnitude of spatial dependency of the evapotranspiration (ET) of Minas Gerais and surround states, estimated by Penman–Monteith (ETo) and Thornthwaite (ETp) methods (mm year^{-1}), mean air temperature (Temp) (°C), precipitation (Prec) (mm year^{-1}), and MODIS evapotranspiration (ET MODIS) (mm year^{-1}), using simple kriging (sk) and simple cokriging (sck) geostatistical analysis

Description	Method			
	sck/ETo	sck/ETp	sk/ETo	sk/ETp
Transformation type	Log	Log	Log	Log
Order of trend removal	Third	Third	First	First
Model type	Spherical	Spherical	Spherical	Spherical
ET	Variogram	Variogram	Variogram	Variogram
Temp	Covariance	Covariance	None	None
Prec	Covariance	Covariance	None	None
ET MODIS	Variogram	Variogram	None	None
Nugget [ET]	0.002124554	0.006570022	0.002670745	0.005839827
Nugget [Tem]	0.001258021	0.001258021		
Nugget [Prec]	0.001340082	0.001340082		
Nugget [ET MODIS]	0.08588594	0.08588594		
Major Range	185,418.1	185,418.1	253,003.5	185,418.1
Partial Sill [ET]	0.00248048	0.006730452	0.004268635	0.01021115
Partial Sill [ET][Temp]	0.0004863111	0.002555286		
Partial Sill [ET][Prec]	−0.001418326	−0.002286813		
Partial Sill [ET][ET MODIS]	−0.00389691	−0.004185068		
Partial Sill [Temp]	0.001966261	0.001966261		
Partial Sill [Temp][Prec]	−0.001278578	−0.001278578		
Partial Sill [Temp][ET MODIS]	0.0001726661	0.0001726661		
Partial Sill [Prec]	0.0109154	0.0109154		
Partial Sill [Prec][ET MODIS]	0.002156619	0.002156619		
Partial Sill [ET MODIS]	0.01990539	0.01990539		
Lag Size	27,735.77	27,735.77	27,735.77	27,735.77
Number of Lags	12	12	12	12

crossed covariance than ETp. MODIS evapotranspiration presented weak pattern of spatial crossed covariance with WorldClim temperature, but strong with WorldClim precipitation. WorldClim temperature and precipitation, as well as the spatial crossed covariance between temperature and precipitation, presented strong structure of spatial dependency. MODIS evapotranspiration itself presented weak pattern of spatial structure of the variogram, with higher nugget variance proportion in relation to the sill (Figs. 4 and 5).

3.3 Simple kriging and cokriging spatial prediction

After the spatial dependency characterization, the spatial prediction of the ETo and ETp was performed by simple kriging, accounting for a single evapotranspiration estimation (Fig. 6), or simple cokriging, accounting for a secondary information, based on the spatial cross-correlation of the co-variables WorldClim temperature, precipitation and

MODIS ET (Fig. 7). The corresponding prediction standard error maps of the simple kriging and simple cokriging were generated. The simple cokriging technique presented satisfactory performance to map the spatial variability of ETo and ETp based on kriging error coefficients, considering that the mean standardized prediction errors and the root-mean square standardized prediction errors presented values near to 0 and 1, respectively, according to ideal conditions of the estimator (Cressie 1993) (Table 3). Observing the standard error maps, it was verified that simple cokriging had better accuracy when compared to the simple kriging spatial prediction. Multivariate geostatistical improvements of detail in the evapotranspiration spatial information were observed. Regarding the spatial variability of the analyzed variables, minor evapotranspiration values occurred over most of the south region of Minas Gerais. In contrast, regions in the north of Minas Gerais presented higher evapotranspiration values (Figs. 6 and 7).
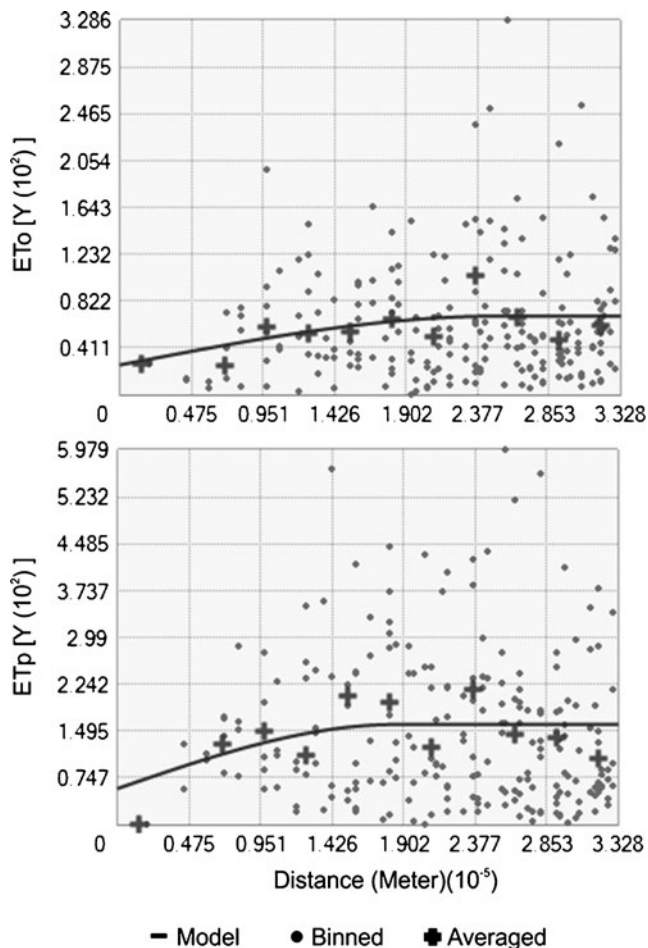
Fig. 3 Evapotranspiration variograms (*Y*) of the Penman–Monteith (*ETo*) and Thornthwaite methods (*ETp*) (mm year^{-1}), used in the simple kriging model, derived from the INMET dataset (1961–1990)

It was observed in the cokriged ETo maps, predominance of subdivisions of climate types between meso-termic and megatermic. However, in the cokriged ETp maps, the magnitude of values was higher, ranging from microtermic to megatermic climate types. Simple kriged maps ranged from mesotermic to magatermic climate types, based on the classification presented in Vianello and Alves (1991).

3.4 Evapotranspiration implementation for the moisture index calculation

The method proposed by Willmott and Feddema (1992) was useful to generate different moisture index maps, based on map algebra calculation in GIS, using WorldClim precipitation (Prec WorldClim) and the different evapotranspiration surfaces derived from simple

kriging Penman–Monteith evapotranspiration (ETo sk), simple kriging Thornthwaite evapotranspiration (ETp sk), simple cokriging Penman–Monteith evapotranspiration (ETo sck), simple cokriging Thornthwaite evapotranspiration (ETp sck), and MODIS evapotranspiration (ET MODIS) (Fig. 8). The moisture index derived from ETo evapotranspiration submitted to simple kriging and simple cokriging presented similar extreme values. In the case of ETp, the simple cokriging presented higher values in the perhumid class, when compared to the simple kriging. However, the simple cokriging defined better the borders of classes with a detailed pattern when compared to the simple kriging. The moisture index derived from MODIS evapotranspiration presented high spatial variation, in great detail, being difficult to observe the dominant process that generated the climate large-scale pattern. Regions in the south of Minas Gerais presented divergence of humid conditions when compared to the moisture index derived from the kriged and cokriged evapotranspiration.

4 Discussion

4.1 Exploratory data analysis

Exploratory data analysis is an integral part of modern statistical practice. In the geostatistical setting, exploratory analysis is naturally oriented towards the preliminary investigation of spatial aspects of the data, which are relevant to check whether the assumptions made by any provisional model were approximately satisfied. When relevant explanatory variables are available at the same data locations of the main considered variables, the explanatory ones can be treated such as additional responses to explain the environmental factors affecting the main variables (Diggle and Ribeiro 2007).

The different ranges in the studied stations with spatial variability of the ETo, ETp, humidity index, mean air temperature, precipitation, and altitude were already expected, considering that Minas Gerais presented extensive mountain ranges with different climate types, as well as evapotranspiration, solar radiation, relative humidity, and wind speed spatial variability (Carvalho et al. 2010; Lemos Filho et al. 2010; Sá Júnior 2011). The difference between the weather station dataset and the high-resolution dataset could be explained by different number of evaluated points and covered range (Fig. 1), as well as to different methods and means of obtaining data. For example, the method for evapotranspiration estimation proposed by Mu et al. (2007a,b) and Allen et al. (1998) are basically the same methods, based

Fig. 4 Variograms (*Y*) covariance and crossed covariance functions (*C*) of the evapotranspiration estimated by Penman–Monteith method (*ETo*) (mmyear^{-1}), temperature (*Temp*) (°C), precipitation (*Prec*) (mmyear^{-1}), MODIS evapotranspiration (*ET MODIS*) (mmyear^{-1}), and the relationship between ETo and Temp, ETo and Prec, ETo and ET MODIS, Temp and Prec, Temp and ET MODIS, and Prec and ET MODIS, used in the simple cokriging model
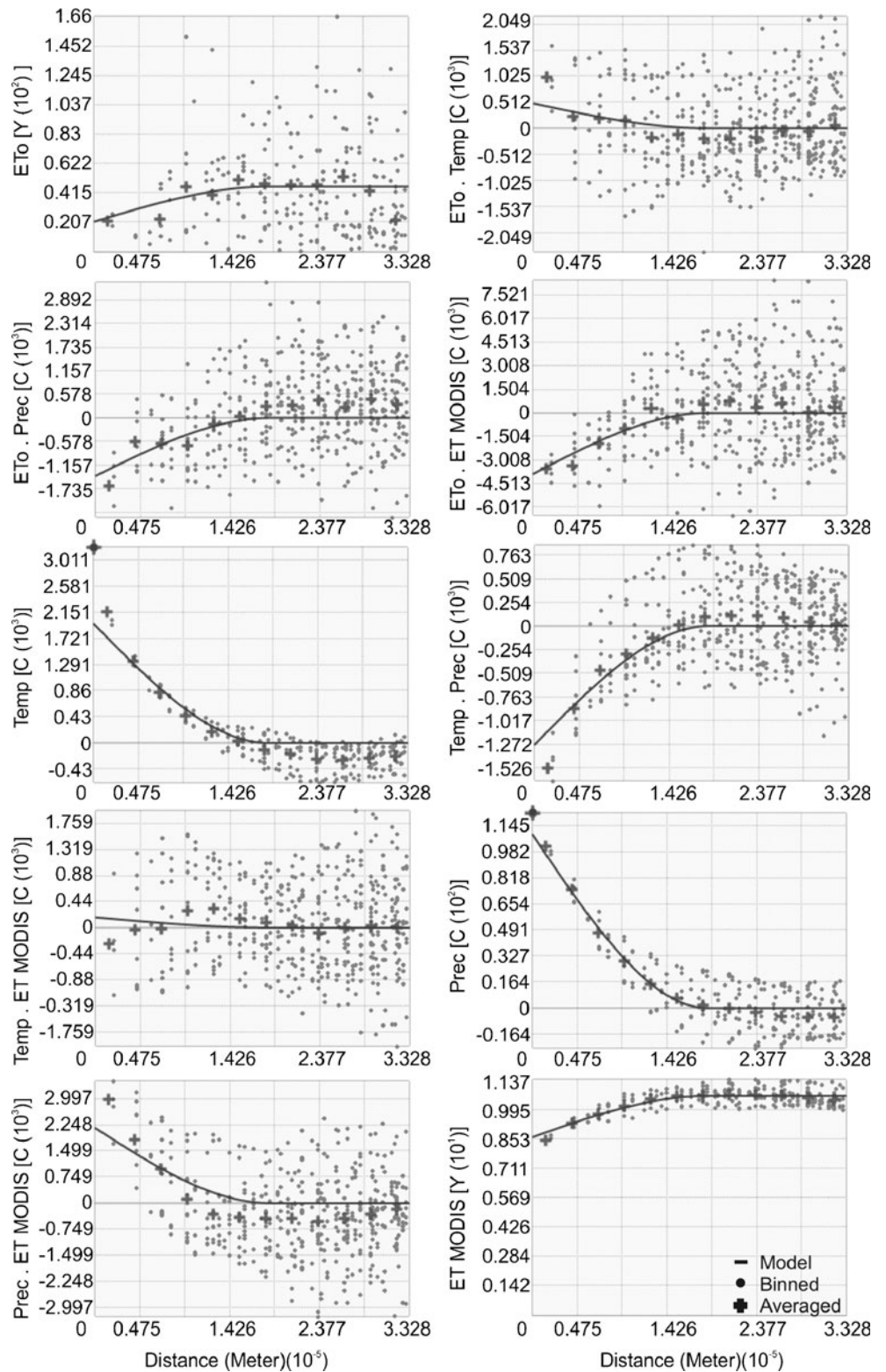
on the Penman–Monteith equation, but with some differences in function of certain conceptual way to get data.

Based on the quintile spatial exploratory plots of the ETo, ETp, and the explanatory variables, mean air temperature,

Fig. 5 Variograms (Y), covariance and crossed covariance functions (C) of the evapotranspiration estimated by the Thornthwaite method (*ETp*) (mmyear^{-1}), temperature (*Temp*) (°C), precipitation (*Prec*) (mmyear^{-1}), MODIS evapotranspiration (ET MODIS) (mmyear^{-1}), and the relationship between ETp and Temp, ETp and Prec, ETp and ET MODIS, Temp and Prec, Temp and ET MODIS, and Prec and ET MODIS, used in the simple cokriging model
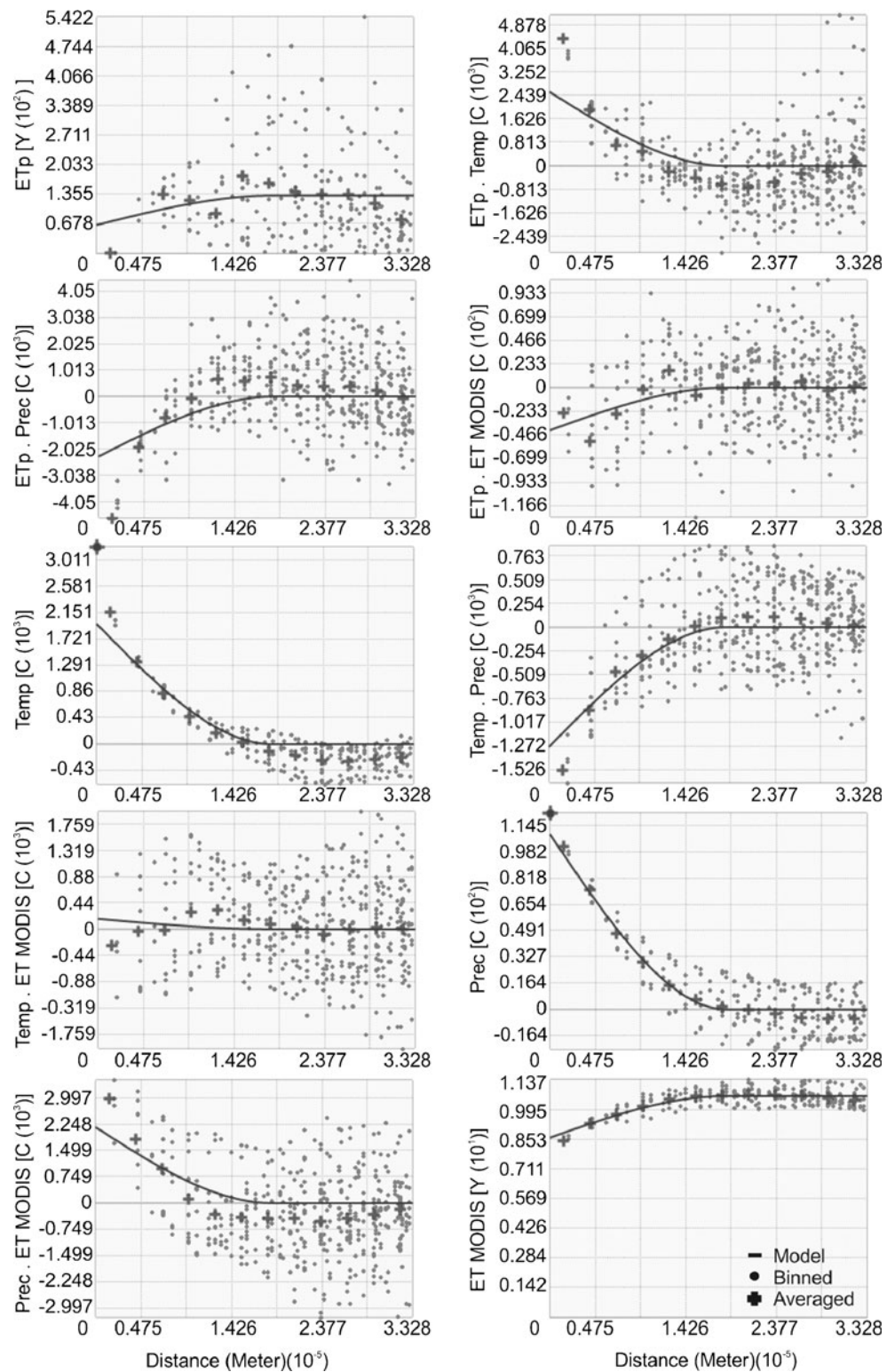
precipitation, Thornthwaite humidity index, and elevation, derived from INMET climatological stations, 1961–1990 period, it was possible to observe the physical environment dependence on longitude, latitude, and altitude, suggesting the inclusion of a trend surface in the model (Fig. 2). Carvalho et al. (2010) also observed the need to include a trend surface model in the simple cokriging analysis to characterize the spatial variability of the humidity index in
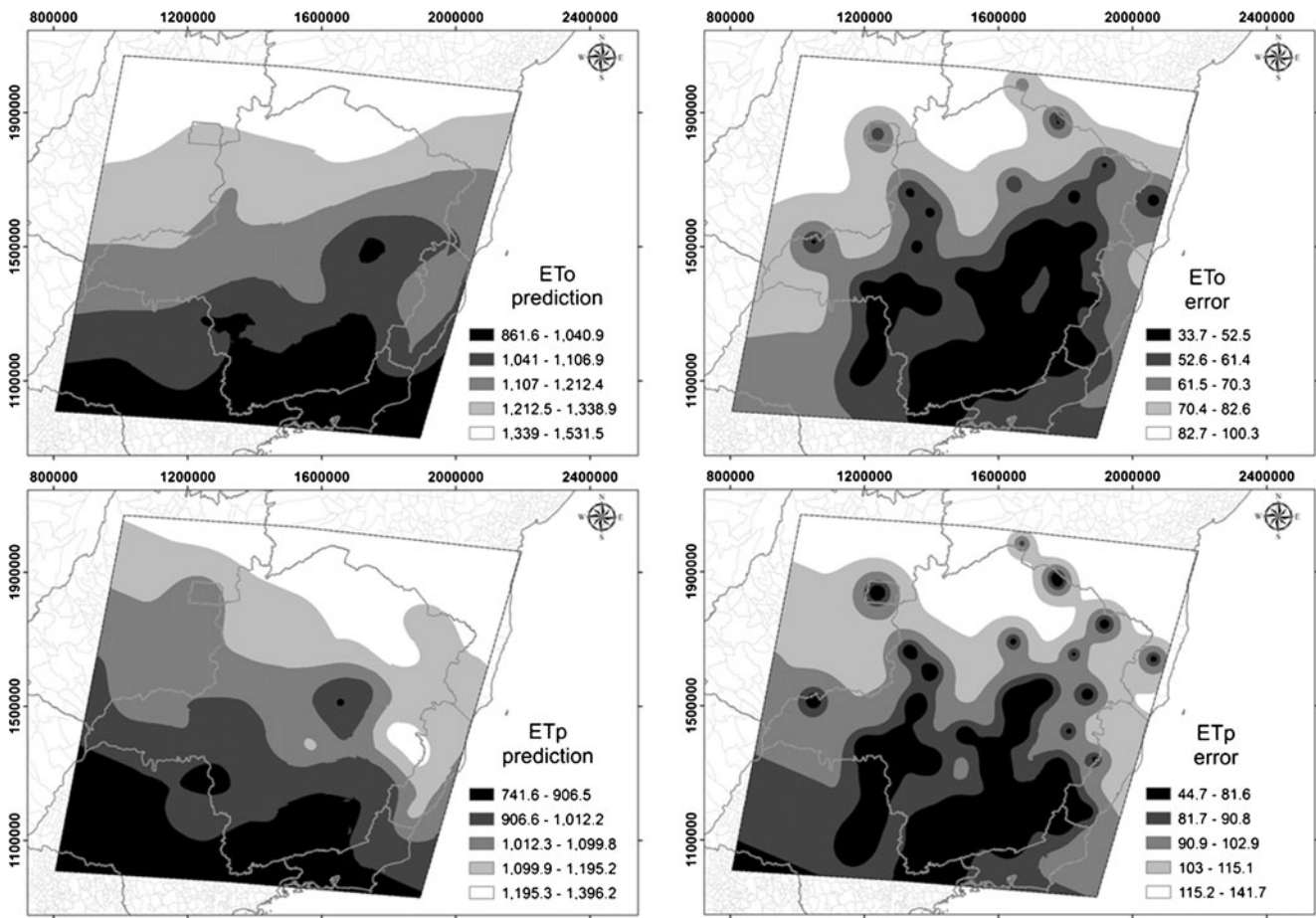
Fig. 6 Simple kriging prediction of the evapotranspiration estimated by Penman–Monteith (*ETo*) and Thornthwaite (*ETp*) methods (mmyear^{-1}) (*left panels*) and the corresponding prediction standard error maps (*right panels*), derived from the INMET dataset (1961–1990)

the Minas Gerais state. In this case, the inclusion of a spatially varying mean in the model was a better modeling strategy for obtaining the typical behavior of a stationary, spatially correlated process, with increase leveling off as the correlation decayed to zero at larger distances.

4.2 Measures of spatial continuity, variability and parameter estimation

The strong spatial crossed covariance between ETo and MODIS evapotranspiration can be explained due to the similar formulation between ETo and MODIS evapotranspiration (Allen et al. 1998; Mu et al. 2007a,b). Otherwise, ETp strong spatial crossed covariance with WorldClim temperature can be explained by the physical-mathematical formulation of the ETo and the greatest number of considered variables when compared to the ETp estimated by the Thornthwaite (1948) approach. Considering that temperature is not sufficient as an indicator of the energy available for the evapotranspiration, higher spatial dependency between evapotranspiration and temperature could generate undesirable erroneous tendencies.

The strong pattern of crossed covariance between evapotranspiration and precipitation rather than temperature indicated that precipitation was a satisfactory explanatory variable of the spatial trends of the evapotranspiration in Minas Gerais state. Beer et al. (2010) observed that the GPP over 40 % of the vegetated land was associated with precipitation. Higher spatial correlations between GPP and precipitation, suggested the existence of missing processes or feedback mechanisms, which attenuate the vegetation response to climate. Teuling et al. (2009) studied the main external drivers of evapotranspiration, related to the incident solar radiation and precipitation. There was strong trend of evapotranspiration correlated with radiation in central Europe, but in central North America, the correlation was weak. In the last situation, trends in precipitation rather than radiation explained trends in evapotranspiration.

The nugget variance proportion in relation to the sill in the MODIS evapotranspiration spatial structure could be related to the high spatial variability of the Earth surface detected by the methodology employed by Mu et al. (2011). In practice, the nugget effect has a dual interpretation as either measurement error or spatial variation on a scale smaller than the smallest distance between any two points in the sample design, or any
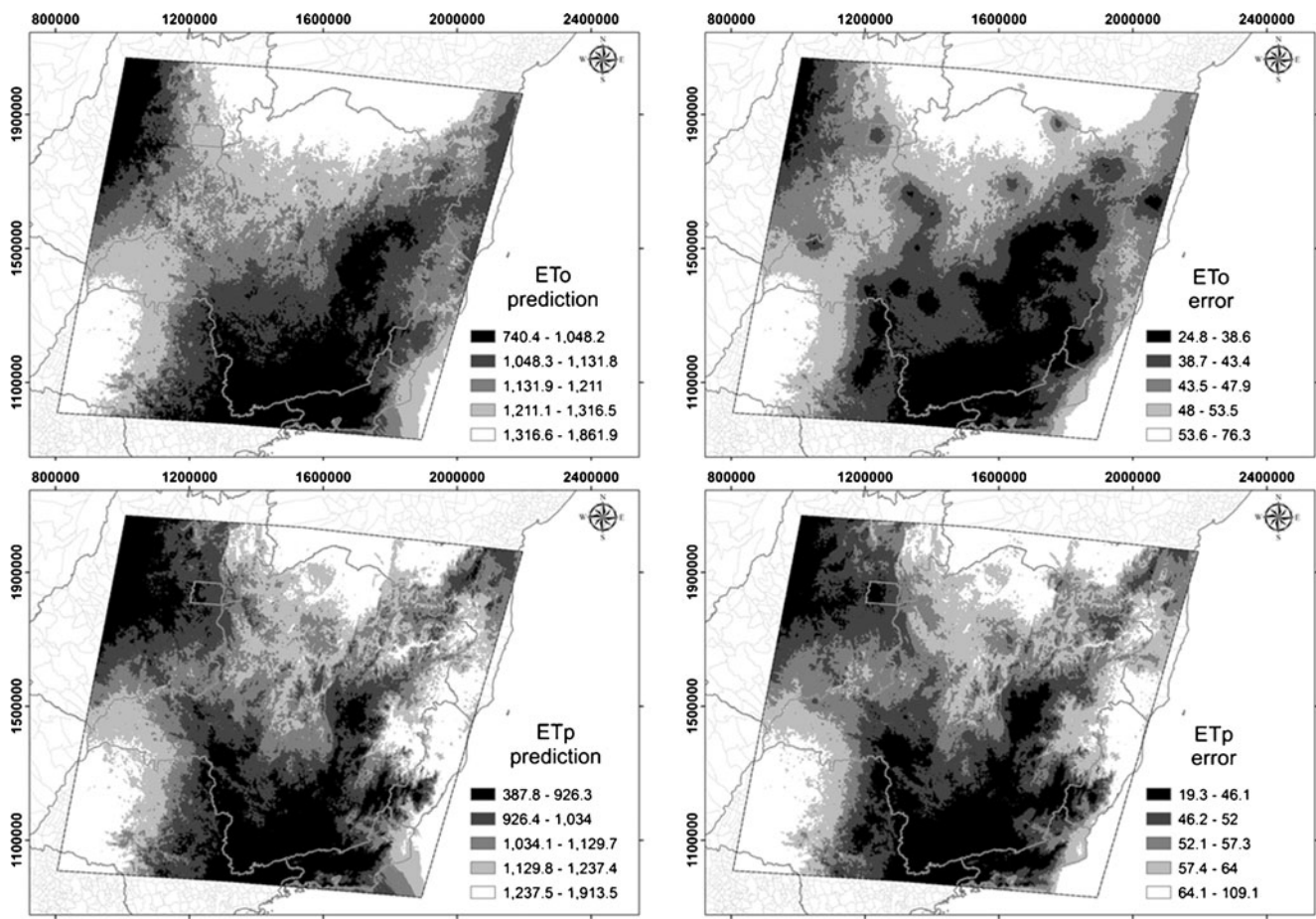
Fig. 7 Simple cokriging prediction of the evapotranspiration estimated by Penman–Monteith (*ETo*) and Thornthwaite (*ETp*) methods (mmyear^{-1}) (*left panels*) and the corresponding prediction standard error maps (*right panels*)

combination of these two effects (Diggle and Ribeiro 2007). Woodcock et al. (1988a), evaluating the extraction of information from remotely sensed simulated images, observed that at small units of regularization, the variograms presented a well-developed drop from the sill in the range of influence. Otherwise, at larger units of regularization, analogous to coarser spatial resolution, the shape of the variogram became very simple. Considering Woodcock et al. (1988a) observations, the MODIS evapotranspiration product with high spatial resolution could reduce the size of the nugget variance and the range, increasing the sill value. However, this situation was not observed, considering the elevated value of the nugget. In this case,

according to Root and Schneider (1995), some of the most conspicuous features observable at smaller scales may not reveal dominant process that generate large-scale patterns. Mechanisms creating larger-scale responses can easily be obscured in noisy or unrelated local variations. This often leads to an inability to detect at small scales a coherent pattern of associations among variables needed for ecological impact assessments at large scales.

4.3 Simple kriging and simple cokriging spatial prediction

Based on the standard error maps, it is possible to observe the better accuracy of the simple cokriging when compared

Table 3 Quality coefficients of the estimates of the simple kriging (sk) and simple cokriging (sck) method used to characterize the evapotranspiration (mmyear^{-1}) of Minas Gerais and surround states by the Penman–Monteith (ETo) and Thornthwaite (ETp) methods

Variable/ method	Samples	Mean prediction error	Root mean square prediction error	Mean standardized prediction error	Root mean square standardized prediction error	Average standard prediction error
ETo/sk	39	1.184712	92.11356	0.002569078	1.070641	87.70006
ETp/sk	39	−1.790814	131.785	−0.02209755	1.053235	126.78
ETo/sck	39	28.72169	114.1812	0.3364307	1.373752	71.09004
ETp/sck	39	29.43903	121.2148	0.1767776	1.280291	103.9878
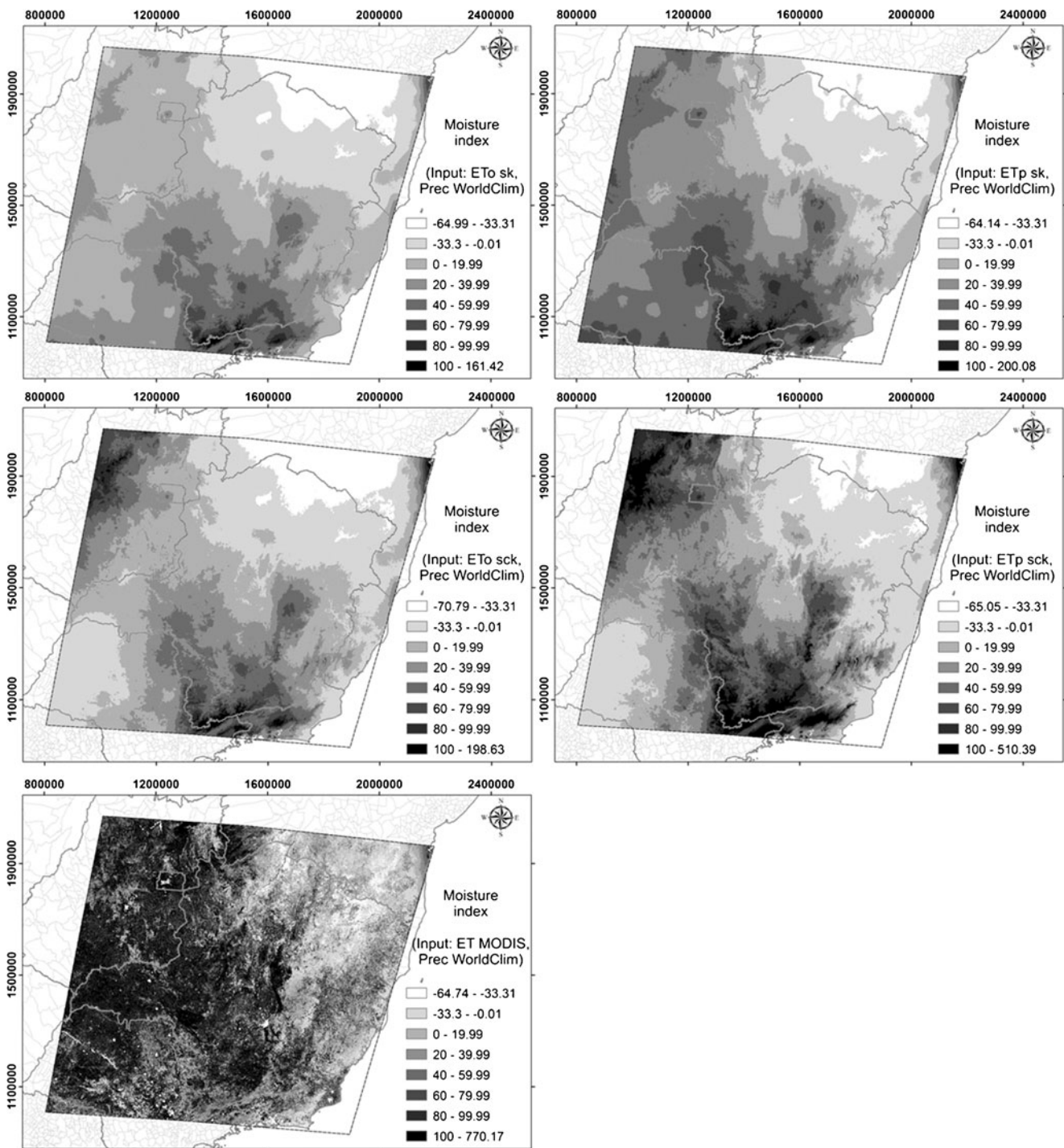
Fig. 8 Moisture index algebra maps derived from WorldClim precipitation (*Prec WorldClim*) and different evapotranspiration products: simple kriging Penman–Monteith evapotranspiration (*ETo sk*), simple kriging Thornthwaite evapotranspiration (*ETp sk*), simple cokriging Penman–Monteith evapotranspiration (*ETo sck*), simple cokriging Thornthwaite evapotranspiration (*ETp sck*), and MODIS evapotranspiration (*ET MODIS*)

to the simple kriging spatial prediction, as well as the multivariate geostatistical detailing improvements of the evapotranspiration spatial information.

This result was expected because Goovaerts (1997) stated that the cokriging estimator is theoretically better than

kriging because its error variance is always smaller than or equal to the error variance of kriging, which ignores all secondary information (Goovaerts 1997).

Martínez-Cob and Cuenca (1992) compared kriging and cokriging prediction errors of evapotranspiration in Oregon,

EUA, and verified higher accuracy of the ordinary cokriging when compared to the kriging method. According to the authors, the disadvantage of the cokriging was related to the high computational effort required. Ashraf et al. (1997) characterizing the spatial pattern of reference evapotranspiration from 17 stations in the states of Nebraska, Kansas, and Colorado, USA, observed better application of cokriging when compared to kriging and inverse distance square methods.

Another advantage of the kriging and cokriging methods is to perform the spatial prediction without bias and with estimation variance less than for any other linear combination of the observed values. Burrough and McDonell (1998) stated that geostatistical methods presented great flexibility for interpolation, providing ways to yield smoothly varying surfaces accompanied by an estimation variance surface, in contrast to the smooth interpolators, which gave a single, local average value. Hijmans et al. (2005) related that the thin-plate smoothing spline algorithm used to generate the high-resolution surfaces of temperature and precipitation, resulted in negative bias under higher elevation and positive bias in the tropics.

ETo and ETp presented, in general, minor evapotranspiration over most of the south region of Minas Gerais, in contrast to higher values in the North of Minas Gerais, with differences determined by the used method for evapotranspiration estimation and the spatial correlation between the WorldClim temperature, precipitation, and MODIS evapotranspiration.

The multivariate geostatistics was a useful tool to characterize the structure and magnitude of spatial dependence of evapotranspiration in Minas Gerais and surrounding states. The methodological approach for evapotranspiration characterization presented in this study can be used as a base for adequate decision making to minimize the risks and negative impacts of climate change in agriculture (Mitchell et al. 2004; Hansen 2002; Lioubimtseva et al. 2005; Rivington et al. 2007; Skirvin et al. 2003) and for the climatic characterization of Minas Gerais state and surrounding regions, based on the obtained spatial variability maps.

As stated by Woodcock et al. (1988b), an improved understanding of the nature and causes of the spatial variation in images would provide a basis for the development of new image techniques and methods, with more logical ways of spatial data using.

4.4 Evapotranspiration implementation for the moisture index calculation

The moisture index derived from the simple kriging evapotranspiration when compared to the simple cokriging, presented differences in magnitude and in the spatial pattern of

the border of the climatic classes. However, the strong trend configured by precipitation in Minas Gerais determined similar spatial patterns of both kriged and cokriged moisture index maps. Acccording to Jung et al. (2010), terrestrial evapotranspiration affected precipitation, and the associated latent heat flux helped to control surface temperature, with important implications for regional climate characteristics such as the intensity and duration of heat waves.

The moisture index derived from the MODIS evapotranspiration presented high spatial variation, in great detail, being difficult to observe the dominant process that generated the climate large-scale pattern.

The regions in the south of Minas Gerais derived from the moisture index estimated with the MODIS evapotranspiration presented divergence of humid conditions when compared to the moisture index derived from the simple kriged and cokriged evapotranspiration, indicating climate change in this region. According to Jung et al. (2010), global annual evapotranspiration increased on average by $7.1 \pm 1 \; \mathrm{mm \, year^{-1} \, decade^{-1}}$ from 1982 to 1997. After that, coincident with the last major El Niño event in 1998, the global evapotranspiration increase seems to have ceased until 2008. Evapotranspiration change was driven primarily by moisture limitation in the Southern Hemisphere, indicating soil moisture decrease from 1998 to 2008. Zhao and Running (2010) also observed that the past decade (2000–2009) has been the warmest since instrumental measurements began. According to the authors, large-scale droughts have reduced regional net primary production (NPP), and a drying trend in the Southern Hemisphere has decreased NPP in that area, counteracting the increased NPP over Northern Hemisphere.

5 Conclusions

The use of geostatistics and the simple cokriging technique enabled the characterization of the spatial variability of the evapotranspiration of Minas Gerais and surrounding states for the average period from 1961 to 1990, using WorldClim temperature, WorldClim precipitation, and MODIS evapotranspiration as covariables, providing uncertainty information on the spatial prediction pattern of the evapotranspiration.

Multivariate geostatistical determined improvements of the spatial information of evapotranspiration weather stations data using high spatial resolution land surface dataset.

ETp values were more influenced by the spatial variability of temperature when compared to ETo, considering the major number of variables in the FAO Penman–Monteith physical–mathematical formulation.

Thorntwaite evapotranspiration presented stronger spatial crossed covariance with WorldClim temperature, than FAO

Penman–Monteith evapotranspiration. There was stronger spatial crossed covariance between FAO Penman–Monteith and MODIS evapotranspiration than Thorntwaite evapotranspiration.

The regions in the south of Minas Gerais derived from the moisture index estimated with the MODIS evapotranspiration (2000–2010), presented divergence of humid conditions when compared to the moisture index derived from the simple kriged and cokriged evapotranspiration (1961–1990), indicating climate change in this region.

There was stronger pattern of crossed covariance between evapotranspiration and precipitation rather than temperature, indicating that trends in precipitation could be one of the main external drivers of the evapotranspiration in Minas Gerais state, Brazil.

References

Allen RG, Pereira LS, Raes D, Smith M (1998) Crop evapotranspiration—guidelines for computing crop water requirements. Food and Agriculture Organization of the United Nations (FAO), Rome

Ashraf M, Loftis JC, Hubbard KG (1997) Application of geostatistics to evaluate partial weather station networks. Agr Forest Meteorol 84:255–271

Atkinson PM, Curran PJ (1995) Defining an optimal size of support for remote sensing investigations. IEEE Trans Geosci Remote Sens 33:768–776

Atkinson PM, Lewis P (2000) Geostatistical classification for remote sensing: an introduction. Comput Geosci 26:361–371

Beer C, Reichstein M, Tomelleri E, Ciais P, Jung M, Carvalhais N, Rödenbeck C, Arain MA, Baldocchi D, Bonan GB, Bondeau A, Cescatti A, Lasslop G, Lindroth A, Lomas M, Luyssaert S, Margolis H, Oleson KW, Roupsard O, Veenendaal E, Viovy N, Williams C, Woodward FI, Papale D (2010) Terrestrial gross carbon dioxide uptake: global distribution and covariation with climate. Science 329:834–838

Brasil (1992) Normais climatológicas (1961–1990). Ministério da Agricultura e Reforma Agrária. Secretaria Nacional de Irrigação, Brasília

Burrough PA, McDonnell RA (1998) Principles of geographical information systems. Oxford University Press, Oxford

Carvalho LG, Alves MC, Oliveira MS, Vianello RL, Sediyama GC, Carvalho LMT (2010) Multivariate geostatistical application for climate characterization of Minas Gerais State, Brazil. Theor Appl Climatol 102:417–428

Chappell A (1998) Using remote sensing and geostatistics to map ^{137}Cs-derived net soil flux in south-west Niger. J Arid Environ 39:441–455

Chilès JP, Delfiner P (2008) Geostatistics: modeling spatial uncertainty. Wiley, Hoboken

Cressie NAC (1985) Fitting variogram models by weighted least squares. Math Geol 17:563–586

Cressie NAC (1993) Statistics for spatial data. Wiley, Hoboken

Curran PJ (1988) The semivariogram in remote sensing: an introduction. Remote Sens Environ 24:493–507

Diggle PJ, Ribeiro PJ Jr (2007) Model-based geostatistics. Springer, New York

Donohue RJ, Roderick ML, McVicar TR (2007) On the importance of including vegetation dynamics in Budyko's hydrological model. Hydrol Earth Syst Sci 11:983–995

Doorenbos J, Pruitt WO (1977) Guidelines for predicting crop water requirements. Food and Agriculture Organization of the United Nations (FAO), Rome

Goovaerts P (1997) Geostatistics for natural resources evaluation. Oxford University Press, Oxford

Goovaerts P (2000) Geostatistical approaches for incorporating elevation into the spatial interpolation of rainfall. J Hidrol 228:113–129

Hansen JW (2002) Realizing the potential benefits of climate prediction to agriculture: issues, approaches, challenges. Agric Syst 74:309–330

Hijmans RJ, Cameron SE, Parra JL, Jones PG, Jarvis A (2005) Very high resolution interpolated climate surfaces for global land areas. Int J Climatol 25:1965–1978

Irmak S, Payero JO, Martin DL, Irmak A, Howell T (2006) Sensitivity analyses and sensitivity coefficients of standardized daily ASCE–Penman–Monteith equation. J Irrig Drain Eng ASCE 132:564–578

Isaaks EH, Srivastava RM (1989) Applied geostatistics. Oxford University Press, Oxford

Jensen JR (2005) Introductory digital image processing: a remote sensing perspective. Pearson Prentice Hall, Upper Saddle River

Jung M, Reichstein M, Ciais P, Seneviratne SI, Sheffield J, Goulden ML, Bonan G, Cescatti A, Chen J, Jeu R, Dolman AJ, Eugster W, Gerten D, Gianelle D, Gobron N, Heinke J, Kimball J, Law BE, Montagnani L, Mu Q, Mueller B, Oleson K, Papale D, Richardson AD, Roupsard O, Running S, Tomelleri E, Viovy N, Weber U, Williams C, Wood E, Zaehle S, Zhang K (2010) Recent decline in the global land evapotranspiration trend due to limited moisture supply. Nature 467:951–953

Lemos Filho LCA, Carvalho LG, Evangelista AWP, Carvalho LMT, Dantas AAA (2007) Spatial-time analysis of evapotranspiration reference in the Minas Gerais State, Brazil. Ciênc Agrotec 31:1462–1469

Lemos Filho LCA, Carvalho LG, Evangelista AWP, Alves Júnior J (2010) Spatial analysis of the influence of meteorological elements on the reference evapotranspiration in the State of Minas Gerais, Brazil. Rev Bras Eng Agríc Ambient 14:1294–1303

Lioubimtseva E, Colea R, Adamsb JM, Kapustin G (2005) Impacts of climate and land-cover changes in arid lands of Central Asia. J Arid Environ 62:285–308

Maillard P (2003) Comparing texture analysis methods through classification. Photogramm Eng Remote Sens 69:357–367

Martínez-Cob A, Cuenca RH (1992) Influence of elevation on regional evapotranspiration using multivariate geostatistics for various climatic regimes in Oregon. J Hydrol 136:353–380

Mather JR, Yoshioka GA (1968) The role of climate in the distribution of vegetation. Ann Assoc Am Geogr 58:29–41

Mitchell N, Espie P, Hankin R (2004) Rational landscape decision-making: the use of meso-scale climatic analysis to promote sustainable land management. Landsc Urban Plan 67:131–140

Mu Q, Zhao M, Heinsch FA, Liu M, Tian H, Running SW (2007a) Evaluating water stress controls on primary production in biogeochemical and remote sensing based models. J Geophys Res 112:1–13

Mu Q, Heinsch FA, Zhao M, Running SW (2007b) Development of a global evapotranspiration algorithm based on MODIS and global meteorology data. Remote Sens Environ 111:519–536

Mu Q, Jones LA, Kimball JS, McDonald KC, Running SW (2009) Satellite assessment of land surface evapotranspiration for the pan-Arctic domain. Water Resour Res 45:1–20

Mu Q, Zhao M, Running SW (2011) Improvements to a MODIS global terrestrial evapotranspiration algorithm. Remote Sens Environ 115:1781–1800

Pereira AR, Villa Nova NA, Sediyama GC (1997) Evapo(transpi)ração. FEALQ, Piracicaba

Rivington M, Matthews KB, Bellocchi G, Buchan K, Stöckle CO, Donatelli M (2007) An integrated assessment approach to conduct analyses of climate change impacts on whole-farm systems. Environ Model Softw 22:202–210

Root TL, Schneider SH (1995) Ecology and climate: research strategies and implications. Science 269:334–341

Sá Júnior A, Carvalho LG, Silva FF, Alves MC (2011) Application of the Köppen classification for climatic zoning in the state of Minas Gerais, Brazil. Theor Appl Climatol 108:1–7

Skirvin SM, Marsh SE, McClaran MP, Meko DM (2003) Climate spatial variability and data resolution in a semi-arid watershed, south-eastern Arizona. J Arid Environ 54:667–686

Smith M (1991) Report on the expert consultation on procedures for revision of FAO guidelines for prediction of crop water requirements. Food and Agriculture Organization of the United Nations (FAO), Rome

Smith M, Allen R, Monteith JL, Perrier A, Pereira LS, Segeren A (1990) Expert consultation on revision of FAO methodologies for crop water requirements. Food and Agriculture Organization of the United Nations (FAO), Rome

Teuling AJ, Hirschi M, Ohmura A, Wild M, Reichstein M, Ciais P, Buchmann N, Ammann C, Montagnani L, Richardson AD, Wohlfahrt G, Seneviratne SI (2009) A regional perspective on trends in continental evaporation. Geophys Res Lett 36:1–5

Thornthwaite CW (1948) An approach towards a rational classification of climate. Geogr Rev 38:55–94

Thornthwaite CW, Mather JR (1955) The water balance. Drexel Institute of Technology, Laboratory of Climatology, Centerton (publications in Climatology, vol. VIII)

Vianello RL, Alves AR (1991) Meteorologia básica e aplicações. Editora UFV, Viçosa

Wackernagel H (2003) Multivariate geostatistics. Springer, New York

Willmott CJ, Feddema JJ (1992) A more rational climatic moisture index. Prof Geogr 44:84–88

Woodcock CE, Strahler AH, Jupp DLB (1988a) The use of variograms in remote sensing: I. Scene models and simulated images. Remote Sens Environ 25:323–348

Woodcock CE, Strahler AH, Jupp DLB (1988b) The use of variograms in remote sensing: II. Real images. Remote Sens Environ 25:349–379

Zhao M, Running SW (2010) Drought-induced reduction in global terrestrial net primary production from 2000 through 2009. Science 329:940–943

Zhao M, Heinsch FA, Nemani RR, Running SW (2005) Improvements of the MODIS terrestrial gross and net primary production global data set. Remote Sens Environ 95:164–176